Iran J Sci Technol Trans Sci (2018) 42:2329–2336
https://doi.org/10.1007/s40995-017-0170-8

RESEARCH PAPER

Heat Analysis in a Nanofluid Layer with Fluctuating Temperature

Morteza Abbasi[1]

Received: 13 September 2016 / Accepted: 23 February 2017 / Published online: 19 April 2017

Abstract In this paper, the time-dependent heat equations over a nanofluid layer are analyzed. The layer is subjected to a fluctuating external temperature on one side and a specified temperature on the other side. The article uses two-phase modeling to formulate the problem and suggests an analytical method for solving the coupled governing partial differential equations of the nanoparticles and base fluid to determine expressions for the base fluid and particle temperature distributions and heat flux. Some of the quantities influencing the non-equilibrium between the nanoparticles and base fluid are investigated in physical aspect. The results show that the non-equilibrium between the nanoparticles and base fluid decreases as the fluctuating temperature's period, volume fraction of nanoparticles and the heat transfer coefficient at the nanoparticle surface increases.

Keywords Nanofluid · Fluctuating temperature · Two-phase model

1 Introduction

Studying the heat transfer process is captivating to many engineers due to its wide range of applications like heat exchangers, fuel cell and electronic devices cooling constructions. As such, enhancement [development] of these processes can save energy and time by lowering the sizes of thermal systems.

✉ Morteza Abbasi
m.abbasi@iausari.ac.ir

1 Department of Mechanical Engineering, Sari Branch, Islamic Azad University, Sari, Iran

To reach this goal, one approach is to enhance fluid flow characteristics—thermal conductivity and thermal diffusivity—which could be achieved by adding nano-size particles of metals, oxides, carbides and carbon to [a] base fluid. This late produced fluid is called nanofluid (Wong and De Leon 2010).

Solid particles have better thermal conductivity compared to conventional base fluids such as pure water, ethylene glycol or oil. The addition of solid nanoparticles increases the thermal conductivity of nanofluids (Abouali and Ahmadi 2012; Afshar et al. 2012). Copper's (Cu) thermal conductivity is a good representative of a solid particle having greater thermal conductivity compared to water or engine oil as pure liquids (Chandrasekaran et al. 2014).

The concept of nanofluids was presented for the first time in 1995 by Choi (Eastman et al. 1995), while Pak and Cho (Pak and Cho 1998) were the first researchers to interpret the application of nanofluids in forced convection heat transfer and observe heat transfer coefficient enhancement of 45 and 75% with 1.34 and 2.78% Al_2O_3 particles in practice. They claimed that for [a] constant average velocity nanofluids, a 3–12% increase in heat transfer coefficient is obtained.

To attain information in calculating nanofluid heat transfer, a nano-layer can be mentioned (Tillman and Hill 2006). Studying non-equilibrium heat conduction in a nanofluid layer with periodic heat flux on one side and a specified temperature on the other side numerically shows that by adding nanoparticles to the base fluid, heat transfer increases (Zhang and Ma 2008).

Recent studies and experiments show that decreasing the size of particles would result in the increase of thermal conductivity. Four probable explanations can be presented, as no existing theory approves this: the particle's Brownian motion; molecular liquid layers formation around the particles; heat transfer nature in the nanoparticle and nanoparticle clustering effect. Due to this observation the generally accepted diffusive transport mechanism is no longer valid at the nanoscale and that the ballistic transport is more realistic (Jang and Choi 2004; Keblinski et al. 2002).

The behavior of a building wall subjected to a Periodic heat, climatic temperature changes, was studied by Strub et al. (2005). The model used to investigate the problem was a solid homogeneous single-phase wall, subjected to a fluctuating external temperature and an ideally constant internal temperature to analyze the total entropy generation over time period and wall thickness.

Timofeeva et al. (2011) presented a summary of systematic experimental studies of both thermophysical and heat transfer in nanofluids. They claimed that the complexity and controversy of nanofluid systems are related to the boundary layers between nanoparticles and the base fluids, resulting in three-phase systems, instead of two-phase ones. They believed that this kind of consideration provides better understanding of the nanofluids.

The potentials of nanofluid application in solar energy systems, such as solar collectors, photovoltaic thermal systems and thermal energy storage systems have been indicated in multiple papers (Hassan et al. 2013; He et al. 2013; Lenert and Wang 2012; Sardarabadi et al. 2014; Yousefi et al. 2012; Zadeh et al. 2015).

Two main methods are utilized to study nanofluids. In the first method called single phase, the base fluid and particles are in thermal and hydrodynamic equilibrium, whereas in the second one, the two-phase model, the base fluid and particles behavior are studied individually. The first model is more popular with the analysts due to its relative simplicity.

The number of the studies using the two-phase modeling of nanofluids is low; therefore, the objective of this paper is to develop the two-phase modeling of studying nanofluids. The two-phase model is used for formulating the problem and an analytical solution is presented to solve it. Hereafter the non-equilibrium between nanoparticles and base fluid is studied by considering a number of physical quantities effect. In industries, when the operating conditions change, the temperature changes with time and fluctuating temperature problems are practical subject.

2 Problem Statement

In this paper, a nanofluid layer with initial temperature of T_i and thickness L is considered. It is suddenly subjected to a fluctuating external temperature on one side and a specified temperature T_B on the other side (Fig. 1).

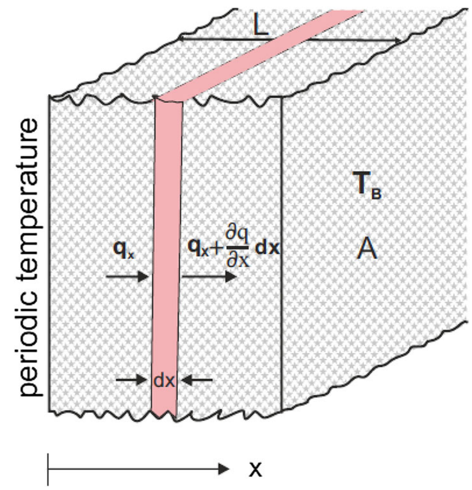

Fig. 1 Schematic representation of the layer and boundary conditions

It is assumed that the layer is thin and free convection is negligible. When the boundary is heated, the heat is first transferred to the base fluid and then the nanoparticles are heated by it. In the physical aspect, there is a time delay between base fluid and particles temperatures.

The heat equation for nanoparticles can be written as:

$$-\left(\rho c_p\right)_s V_s \frac{\partial T_s}{\partial t} = A_s h_s (T_s - T_f). \tag{1}$$

The subscripts s and f are used for fluid and nanoparticle quantity, respectively. The V_s, A_s and h_s are total volume, total surface of nanoparticles and heat transfer coefficient at the nanoparticle surface, respectively.

In Eq. (1),

$$A_s = nA'_s, v_s = nv'_s. \tag{2}$$

The V'_s, A'_s and n are nanoparticle volume, nanoparticle surface and total number of nanoparticles. The coupling factor G and volume fraction of nanoparticles φ are defined as:

$$G = \frac{\varphi A_s h_s}{V_s}, \tag{3}$$

$$\varphi = \frac{V_s}{V_{nf}} = \frac{V_s}{V_s + V_f}. \tag{4}$$

The subscript nf is used for nanofluid quantity. By using (2–4) in (1), the heat equation for nanoparticles is obtained as (Zhang 2006):

$$\varphi\left(\rho c_p\right)_s \frac{\partial T_s}{\partial t} = G(T_f - T_s). \tag{5}$$

In Fig. 1 for the volume element of thickness dx, the following energy balance may be made which gives the heat equation for the base fluid:

$$-\left(\rho c_p\right)_f dV_f \frac{\partial T_f}{\partial t} = nA_s h_s (T_f - T_s) + \frac{\partial q_x}{\partial x} dx, \tag{6}$$

in which:

$$\begin{aligned} dV_{\mathrm{f}} &=(1-\varphi)dV_{\mathrm{nf}}=(1-\varphi)Adx,\\ q_{\mathrm{x}} &=-k_{\mathrm{nf}}A\frac{\partial T_{\mathrm{f}}}{\partial x},\\ n &=\frac{\varphi dV_{\mathrm{nf}}}{V_{\mathrm{s}}}=\frac{\varphi}{V_{\mathrm{s}}}Adx, \end{aligned} \tag{7}$$

where V_{f} is base fluid volume. Combining (6) and (7) gives

$$-\left(\rho c_{\mathrm{p}}\right)_{\mathrm{f}}(1-\varphi)\frac{\partial T_{\mathrm{f}}}{\partial t}=\frac{\varphi}{v_{\mathrm{s}}}A_{\mathrm{s}}h_{\mathrm{s}}(T_{\mathrm{f}}-T_{\mathrm{s}})-k_{\mathrm{nf}}\frac{\partial^2 T_{\mathrm{f}}}{\partial x^2}. \tag{8}$$

By using (3) in (8), the heat equation for base fluid is obtained as (Zhang and Ma 2008):

$$(1-\varphi)\left(\rho c_{\mathrm{p}}\right)_{\mathrm{f}}\frac{\partial T_{\mathrm{f}}}{\partial t}=k_{\mathrm{nf}}\frac{\partial^2 T_{\mathrm{f}}}{\partial x^2}+G(T_{\mathrm{s}}-T_{\mathrm{f}}). \tag{9}$$

The initial and boundary conditions for problem are:

$$T_{\mathrm{s}}(x,0)=T_{\mathrm{f}}(x,0)=T_i, \tag{10}$$

$$T_{\mathrm{f}}(0,t)=T_{\mathrm{i}}+(T_{\mathrm{B}}-T_{\mathrm{i}})\lambda\sin\left(\frac{2\pi t}{t_{\mathrm{p}}}\right),\quad atx=0, \tag{11}$$

$$T_{\mathrm{f}}(L,t)=T_{\mathrm{B}},\quad atx=L, \tag{12}$$

where λ and t_{p} are altitude and period of fluctuating temperature.

Some non-dimensional parameters are defined as (Zhang and Ma 2008):

$$\begin{aligned} \theta &=\frac{(T-T_{\mathrm{i}})}{(T_{\mathrm{B}}-T_{\mathrm{i}})};X=\frac{x}{L};\tau=\frac{\alpha_f t}{L^2};\\ C_{\mathrm{sf}} &=\frac{(\rho c_{\mathrm{p}})_{\mathrm{s}}}{(\rho c_{\mathrm{p}})_{\mathrm{f}}},K_{\mathrm{eff}}=\frac{k_{\mathrm{nf}}}{k_{\mathrm{f}}},Sp=\frac{GL^2}{\varphi k_{\mathrm{f}}}. \end{aligned} \tag{13}$$

In these expressions, Sp is Sparrow number, k_{eff} and C_{sf} are called dimensionless effective thermal conductivity and heat capacity ratio, respectively.

By using non-dimensional parameter in heat equations, we have

$$C_{\mathrm{sf}}\frac{\partial\theta_{\mathrm{s}}}{\partial\tau}=Sp(\theta_{\mathrm{f}}-\theta_{\mathrm{s}}), \tag{14}$$

$$(1-\varphi)\frac{\partial\theta_{\mathrm{f}}}{\partial\tau}=K_{\mathrm{eff}}\frac{\partial^2\theta_{\mathrm{f}}}{\partial X^2}+\varphi Sp(\theta_{\mathrm{s}}-\theta_{\mathrm{f}}). \tag{15}$$

Using non-dimensional parameter in boundary and initial conditions yields:

$$\theta_{\mathrm{s}}(X,0)=\theta_{\mathrm{f}}(X,0)=0, \tag{16}$$

$$\theta_{\mathrm{f}}(0,\tau)=\lambda\sin\left(\frac{2\pi\tau}{\tau_{\mathrm{p}}}\right), \tag{17}$$

$$\theta_{\mathrm{f}}(L,\tau)=1. \tag{18}$$

For simplicity, in this paper we suppose the interfacial resistance of nanoparticle surface is negligible and in this special case k_{eff} can be formulated (Evans et al. 2006; MacDevette et al. 2013):

$$k_{\mathrm{eff}}=1+3\varphi. \tag{19}$$

3 Analytical Solutions

The partial differential Eqs. (14) and (15) are transformed to a system of ordinary differential equations by using sine transform definition.

The Fourier sine transform of the function $\theta(X,\tau)$ on interval [0, 1] is defined as (Kreyszig et al. 2011):

$$F_{\mathrm{s}}[\theta(X,\tau)]=2\int_0^1\sin(n\pi X)\theta(X,\tau)dX=S_{\mathrm{n}}(\tau). \tag{20}$$

Then $\theta(X,\tau)$ can be achieved as:

$$\theta(X,\tau)=\sum_{n=1}^{\infty}S_n(t)\sin(n\pi X). \tag{21}$$

It is shown that:

$$F_{\mathrm{s}}\left(\frac{\partial^2(\theta,\tau)}{\partial X^2}\right)=-\left(\frac{n\pi}{L}\right)^2 S_n(=\tau)+\frac{2n\pi}{L^2}\left[\theta(0,\tau)+(-1)^{n+1}\theta(L,\tau)\right]. \tag{22}$$

By using transform definition and its properties as shown above, the final heat equations and their conditions Eqs. (14)–(18) can be written as:

$$C_{\mathrm{sf}}\frac{ds_{\mathrm{n}}^{\mathrm{s}}}{d\tau}=Sp\left(s_{\mathrm{n}}^{\mathrm{f}}-s_{\mathrm{n}}^{\mathrm{s}}\right), \tag{23}$$

$$\begin{aligned}(1-\varphi)\frac{ds_{\mathrm{n}}^{\mathrm{f}}}{d\tau}=K_{\mathrm{eff}}\left\{-(n\pi)^2S_n^{\mathrm{f}}(\tau)+2n\pi\left[\lambda\sin\left(\frac{2\pi\tau}{\tau_{\mathrm{p}}}\right)+(-1)^{n+1}\right]\right\}\\ +\varphi Sp\left(s_{\mathrm{n}}^{\mathrm{s}}-s_{\mathrm{n}}^{\mathrm{f}}\right),\end{aligned} \tag{24}$$

$$S_{\mathrm{n}}^{\mathrm{s}}(0)=0,S_{\mathrm{n}}^{\mathrm{f}}(0)=0. \tag{25}$$

The computation software Maple V.14 is used to solve the system of ordinary Eqs. (23) and (24) with the boundary conditions (25) for some values of physical quantity, the functions of $s_{\mathrm{n}}^{\mathrm{f}}$ and $s_{\mathrm{n}}^{\mathrm{s}}$ are obtained. Then the final solution, dimensionless temperature distributions are obtained as:

$$\theta_{\mathrm{f}}(X,\tau)=\sum_{n=1}^{j}S_{\mathrm{n}}^{\mathrm{f}}(\tau)\sin(n\pi X), \tag{26}$$

$$\theta_{\mathrm{s}}(X,\tau)=\sum_{n=1}^{j}S_{\mathrm{n}}^{\mathrm{s}}(\tau)\sin(n\pi X). \quad (27)$$

The heat flux q'' at any point x_{a} and the transferred heat q_{m} at any interval $[m\tau_{\mathrm{p}},(m+1)\tau_{\mathrm{p}}]$ can be achieved as:

$$q''(t)=-k_{\mathrm{nf}}\frac{\partial T_{\mathrm{f}}(x,t)}{\partial x}\bigg|_{x_{\mathrm{a}}}, \quad (28)$$

$$\frac{q_{\mathrm{m}}}{A}=\int_{m\,t_{\mathrm{p}}}^{(m+1)t_{\mathrm{p}}}q''(t)\mathrm{d}t. \quad (29)$$

By introducing dimensionless heat transferred parameter as:

$$Q'_{\mathrm{m}}=\frac{q_{\mathrm{m}}LA}{k_{\mathrm{nf}}(T_{\mathrm{B}}-T_{\mathrm{i}})t_{\mathrm{p}}},$$

and using non-dimensional parameters Eq. (13), Eq. (29) is rearranged as:

$$Q'_{\mathrm{m}}=-\int_{m}^{(m+1)}\frac{\partial\theta_{\mathrm{f}}(X,\tau/\tau_{\mathrm{p}})}{\partial X}\bigg|_{X_{\mathrm{a}}}d(\tau/\tau_{\mathrm{p}}). \quad (30)$$

The dimensionless total heat transferred at any point X_{a} for interval $[0,(m+1)\tau/\tau_{\mathrm{p}}]$ can achieve

$$Q=\sum_{m=1}^{m+1}Q'_{\mathrm{m}}. \quad (31)$$

Table 1 Comparison of Analytical and numerical results

τ/τ_{p}	$\theta_{\mathrm{Analytical}}$		$\theta_{\mathrm{Numerical}}$		Error$(\lvert\theta_{\mathrm{Analytical}}-\theta_{\mathrm{Numerical}}\rvert)$	
	$X_{\mathrm{f}}=0.1$	$X_{\mathrm{s}}=0.1$	$X_{\mathrm{f}}=0.1$	$X_{\mathrm{s}}=0.1$	$X_{\mathrm{f}}=0.1$	$X_{\mathrm{s}}=0.1$
0.5	0.73023	0.228739	0.730229	0.228839	6.00E–05	1.00E–04
1	−0.43677	0.136847	−0.43677	0.136889	0.00E00	4.2E–05
1.5	0.591471	0.129669	0.591471	0.129689	0.00E00	2.00E–05
2	−0.49197	4.81E−02	−0.49197	4.81E−02	0.00E00	0.00E00
2.5	0.562863	7.16E–02	0.562863	7.16E–02	0.00E00	0.00E00
3	−0.50886	1.23E–02	−0.50886	1.23E–02	0.00E00	0.00E00
3.5	0.552351	4.96E–02	0.552351	4.96E–02	0.00E00	0.00E00
4	−0.51532	−1.24E–03	−0.51532	−1.23E–03	0.00E00	1.00E–05
4.5	0.548773	4.14E–02	0.548773	4.14E–02	0.00E00	0.00E00
5	−0.51672	−5.88E–03	−0.51672	−5.87E–03	0.00E00	1.00E–05

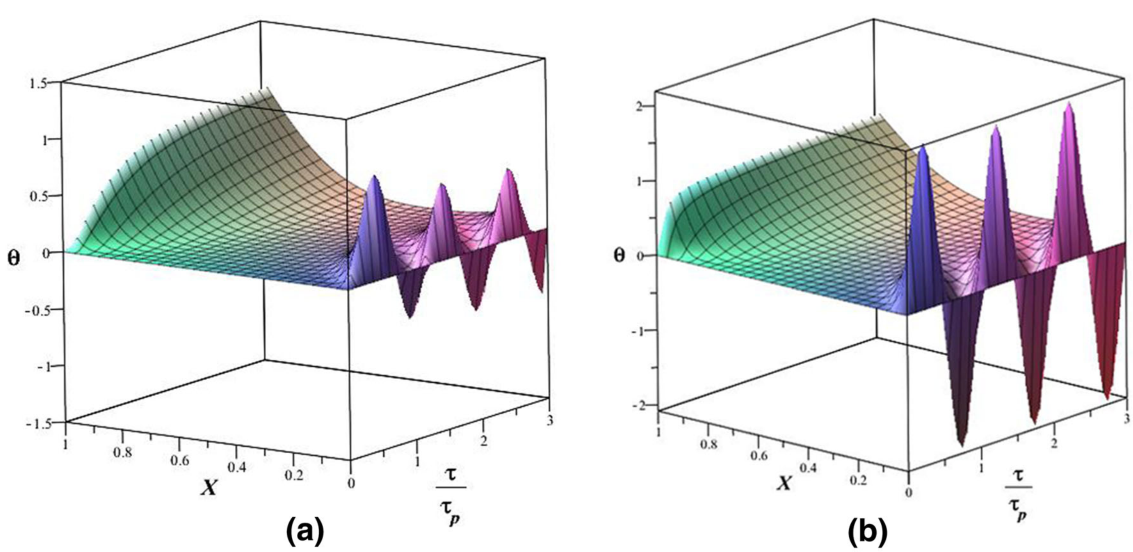

Fig. 2 Dimensionless temperature distributions for the special case $(sp=500,\tau_{\mathrm{p}}=0.01,\varphi=0.02)$: **a** base fluid, **b** nanoparticle

4 Results and Discussion

For validity, the problem was solved numerically, 4th order Runge–Kutta, for the special case $Sp = 500, \phi = 0.002, \tau_p = 0.01$. Comparison showed that there is an excellent agreement between analytical and numerical results that is shown in Table 1. As mentioned in the previous section, the temperature distribution is achieved in several cases for special values of physical quantities. For all solved cases λ and C_{sf} values are selected 3 and 2.7, respectively. The solutions are shown graphically, because they are too long to be presented here. For reader's physical consideration, spatial graphs are drawn for special cases $(sp = 500, \tau_p = 0.01 \text{ and } \varphi = 0.02)$ as shown in Fig. 2.

But to analyze the results, solutions should be presented in two-dimensional diagrams. In all the two-dimensional diagrams, continuous line and dashed symbol are used for base fluid and nanoparticle temperature distributions, respectively.

For $(Sp = 500, \varphi = 0.02)$ the equations are solved at different values of τ_p and Figs. 3 and 4 are prepared in order to investigate the effect of fluctuating period on response. It can be seen that by increasing τ_p, the non-equilibrium between the nanoparticles and base fluid decreases. In physical aspects when τ_p increases (frequency decreases), the particles have more time to approach the base fluid temperature.

For $(\tau_p = 0.01, \varphi = 0.02)$ the equations are solved at different values of Sp and Fig. 5 is prepared in order to investigate the effect of Sparrow number on the response. It can be seen that the non-equilibrium between the nanoparticles and base fluid decreases with the increase of Sp. The sparrow number is proportional to h_s (the heat transfer coefficient at the nanoparticle surface), so by increasing Sp the heat transfer rate between nanoparticles and base fluid increases, contact resistances decreases and non-equilibrium effect is reduced. In the limiting case, when contact resistance approaches to zero, the non-equilibrium vanishes.

For $(\tau_p = 0.01, sp = 500)$ the equations are solved at different values of φ, volume fraction of nanoparticles and Fig. 6 are prepared in order to investigate the effect of volume fraction on response. It can be seen that the temperature fluctuating amplitude in the layer and non-equilibrium effect is increased when φ increases. When φ increases the number of nanoparticles in fluid is increased, as well as nanofluid conductivity and heat diffusion. It means that the heat penetration in nanofluids goes up and fluctuating boundary temperature has a bigger effect on the layer temperature distribution.

Besides, in all cases at a significant time after starting the process, the temperature of nanoparticles approached that of the base fluid at the constant temperature layer side.

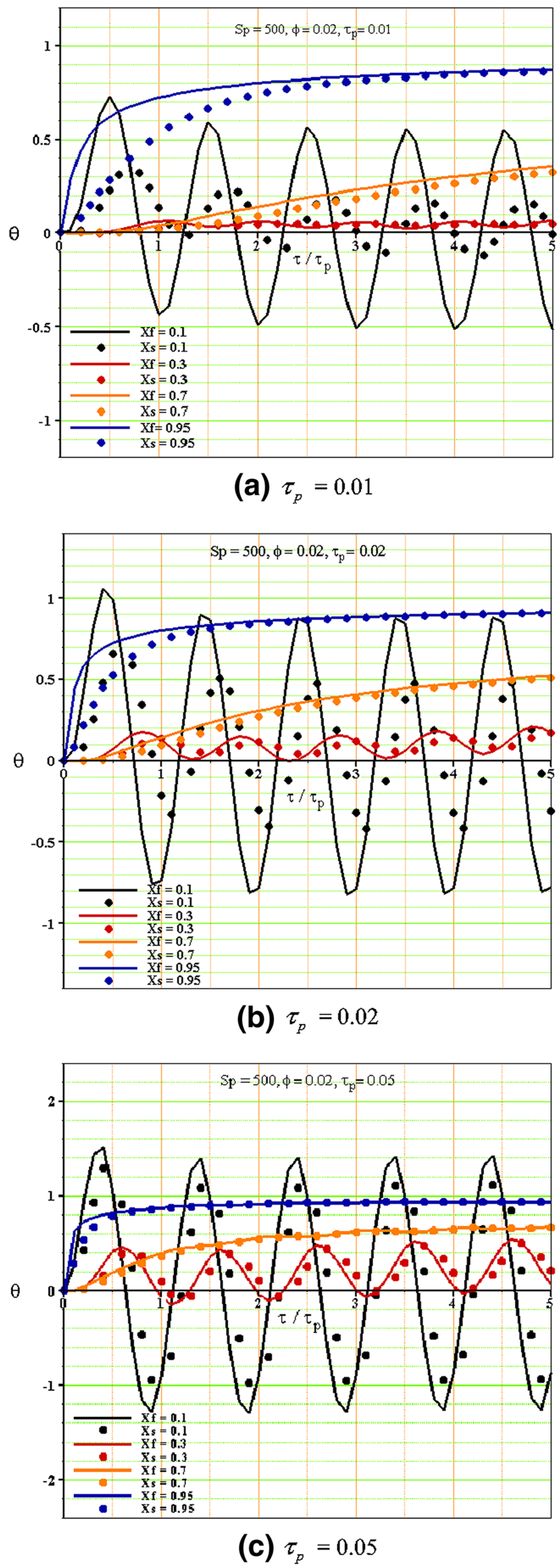

Fig. 3 Dimensionless temperature distributions for different values of τ_p at several X. **a** $\tau_p = 0.01$, **b** $\tau_p = 0.02$, **c** $\tau_p = 0.05$

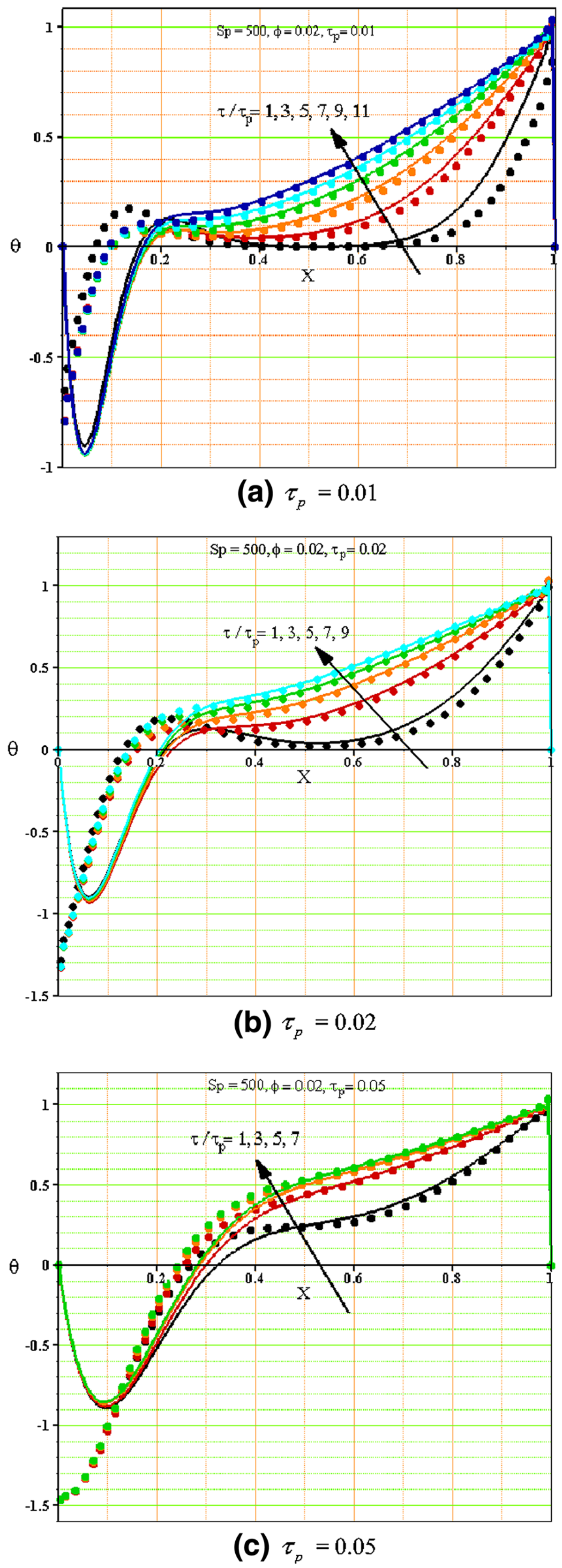

Fig. 4 Dimensionless temperature distributions for different values of τ_p at several τ/τ_p. **a** $\tau_p = 0.01$, **b** $\tau_p = 0.02$, **c** $\tau_p = 0.05$

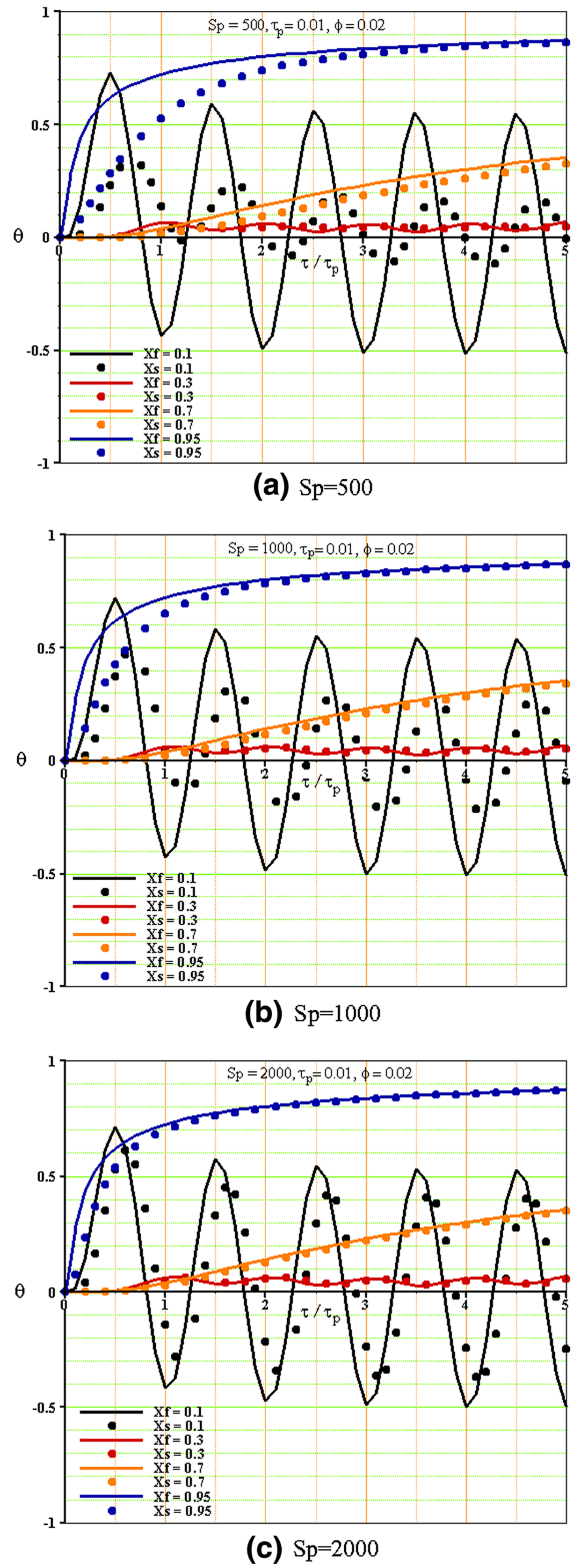

Fig. 5 Dimensionless temperature distributions for different values of *sp* at several *X*. **a** *Sp* = 500, **b** *Sp* = 1000, **c** *Sp* = 2000

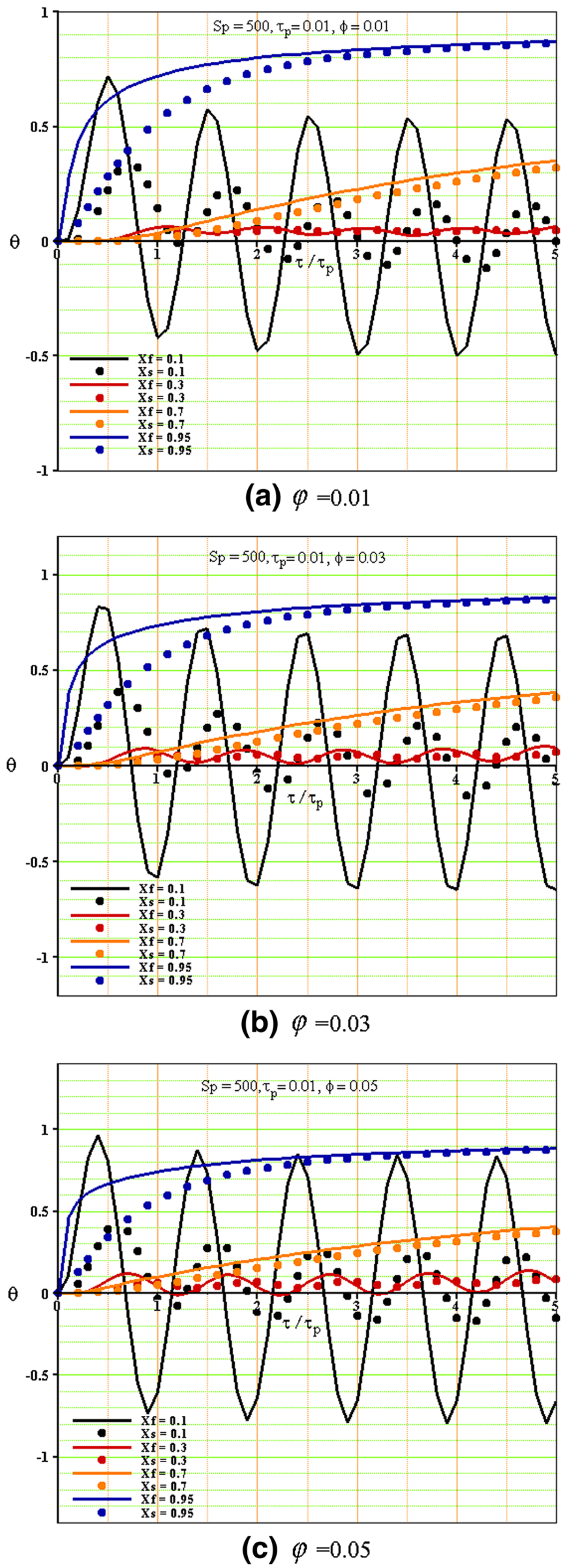

Fig. 6 Dimensionless temperature distributions for different values of φ at several X. **a** $\varphi = 0.01$, **b** $\varphi = 0.03$, **c** $\varphi = 0.05$

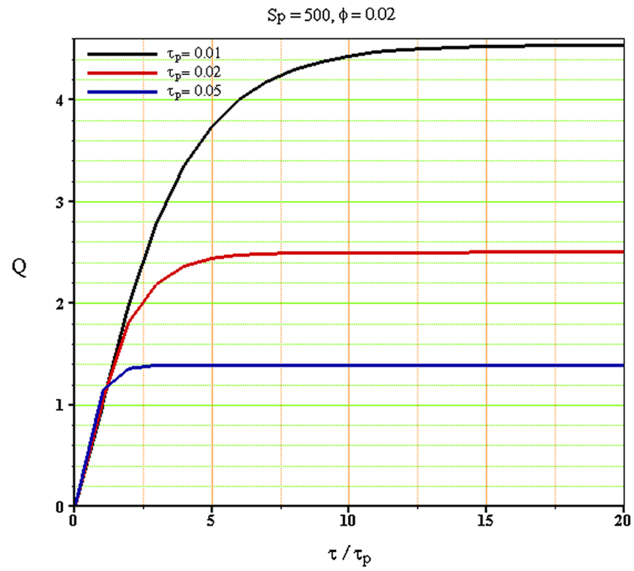

Fig. 7 Dimensionless total heat transfer behavior

This behavior is not seen at the other side where the temperature fluctuates with time.

As an example, using Eq. (31) dimensionless total heat transferred Q is calculated and for special cases $(sp = 500, \varphi = 0.02)$ at $X_a = 0.5$ is drawn in Fig. 7.

It can be seen that Q approaches to some value and remains constant after a couple of fluctuating. It means that after an adequate time, temperature fluctuates in a way that the heat flowing on the right side is equal to the one on the left side inside the two halves of a cycle. It can be seen that by increasing τ_p the approached value decreases.

5 Conclusions

In this article, an analytical method is offered for solving the partial differential equations of a nanofluid layer which is formulated by the two-phase model. The layer is subjected to a fluctuating external temperature on one side and a specified temperature on the other side. The non-dimensional temperature distribution for base fluid and nanoparticles is obtained. The results show that the non-equilibrium between the nanoparticles and base fluid decreases with the increase of the fluctuating temperature's period, the volume fraction of nanoparticles and the heat transfer coefficient at the nanoparticle surface.

References

Abouali O, Ahmadi G (2012) Computer simulations of natural convection of single phase nanofluids in simple enclosures: a critical review. Appl Therm Eng 36:1–13

Afshar H, Shams M, Nainian SMM, Ahmadi G (2012) Two-phase study of fluid flow and heat transfer in gas-solid flows (nanofluids). Appl Mech Mater 110–116:3878–3882

Chandrasekaran P, Cheralathan M, Kumaresan V, Valraj R (2014) Enhanced heat transfer characteristics of water based copper oxide nanofluid PCM (phase change material) in a spherical capsule during solidification for energy efficient cool thermal storage system. Energy 72:636–642

Eastman JA, Choi US, Li S, Thompson LJ, Lee S (1995) Enhancing thermal conductivity of fluids with nanoparticles, developments and applications of non-newtonian flows. Illinois. UNT Digital Library

Evans W, Fish J, Keblinski P (2006) Role of Brownian motion hydrodynamics on nanofluid thermal conductivity. Appl Phys Lett 88(9):1–3

Hassan M, Sadri R, Ahmadi G, Dahari MB, Kazi SN, Safaei MR, Sadeghinezhad E (2013) Numerical study of entropy generation in a flowing nanofluid used in micro-and minichannels. Entropy 15(1):144–155

He Q, Wang S, Zeng S, Zheng Z (2013) Experimental investigation on photothermal properties of nanofluids for direct absorption solar thermal energy systems. Energy Convers Manag 73:150–157

Jang SP, Choi SUS (2004) Role of Brownian motion in the enhanced thermal conductivity of nanofluids. Appl Phys Lett 84(21):4316–4318

Keblinski P, Phillpot SR, Choi SUS, Eastman JA (2002) Mechanisms of heat flow in suspension of nano-sized particles (nanofluids). Int J Heat Mass Transf 45(4):855–863

Kreyszig E, Kreyszig H, Norminton EJ (2011) Advanced engineering mathematics. Wiley, Jefferson

Lenert A, Wang N (2012) Optimization of nanofluid volumetric receivers for solar thermal energy conversion. Sol Energy 86(1):253–265

MacDevette MM, Ribera H, Myers TG (2013) A simple yet effective model for thermal conductivity of nanofluids. Centre De Recerca Matematica, pp 1–20

Pak BC, Cho Y (1998) Hydrodynamic and heat transfer study of dispersed fluids with submicron metallic oxide particles. Exp Heat Transf 11(2):151–170

Sardarabadi M, Passandideh-Fard M, Heris SZ (2014) Experimental investigation of the effects of silica/water nanofluid on PV/T (Photovoltaic thermal units). Energy 66:264–272

Strub F, Castaing-Lasvignottes J, Strub M, Pons Michel, Monchoux F (2005) Second Law analysis of periodic heat conduction through a wall. Int J Therm Sci 44:1154–1160

Tillman P, Hill JM (2006) A new model for thermal conductivity in nanofluids. In: Jagadish C, Lu G (eds) Proceedings of 2006 international conference on nanoscience and nanotechnology, pp 673–676

Timofeeva EV, Yu W, France DM, Singh D, Routbort JL (2011) Nanofluids for heat transfer: an engineering approach. Nanoscale Res Lett 6(182):1–7

Wong KV, De Leon O (2010). Applications of nanofluids: current and future. Adv Mech Eng

Yousefi T, Veysi F, Shojaeizadeh E, Zinadini S (2012) An experimental investigation on the effect of Al_2O_3–HO nanofluid on the efficiency of flat-plate solar collectors. Renew Energy 39(1):293–298

Zadeh PM, Sokhansefat T, Kasaeian AB, Kowsary F, Akbarzadeh A (2015) Hybrid optimization algorithm for thermal analysis in a solar parabolic trough. Energy 82:857–864

Zhang Y (2006) Nonequilibrium modeling of heat transfer in a gas-saturated powder layer subject to a short-pulsed heat source. Numer Heat Transfer Part A 50(6):509–524

Zhang Y, Ma HB (2008) Nonequilibrium heat conduction in a nanofluid layer with periodic heat flux. Int J Heat Mass Transf 51(19–20):4862–4874